Inflated Cone Experiment for High-Throughput Characterization of Time-Dependent Polymer Membranes

Veli Bugra Ozdemir
Department of Mechanical and Aerospace Engineering,
University of Central Florida,
Orlando, FL 32816
e-mail: vbugra@knights.ucf.edu

Kawai Kwok[1]
Assistant Professor
Department of Mechanical and Aerospace Engineering,
University of Central Florida,
Orlando, FL 32816
e-mail: kawai.kwok@ucf.edu

Long-term behavior of polymer membranes in the nonlinear regime is probed by strain histories under various stress levels. Current characterization methods for polymer membranes impose a uniform stress field and hence require a series of long-duration tests to be conducted, which poses a significant experimental challenge. Here, we present the inflated cone method to generate a continuous spectrum of strain histories under various stresses in a single experiment. By imposing a known stress gradient and utilizing a full-field strain measurement technique, the inflated cone method provides a high-throughput approach for extracting time-dependent data of polymer membranes. The method is suitable for studying nonlinear time-dependent deformations under a biaxial stress state. The stress range and ratio can be easily modulated by cone geometry design. We demonstrate the utility of the method through creep-recovery tests carried out on a polyethylene thin film. The proposed experimental method is highly beneficial for the development of nonlinear viscoelastic and viscoplastic models.
[DOI: 10.1115/1.4054523]

Keywords: constitutive modeling of materials, mechanical properties of materials, stress analysis, structures

1 Introduction

Tensioned polymer membranes can be used as structural supports or reflecting surfaces for large and lightweight aerospace structures such as superpressure balloons [1], inflatable spacecraft booms [2], solar sails [3], and satellite reflector antennas [4]. These structures operate for long periods of time under varying temperatures, where the membranes are subjected to large deformation. Acquiring empirical data on the time-dependent response of the polymer membranes is critical for successful analysis and design.

An ongoing challenge in this regard is the immensely time-consuming characterization process of the long-term mechanical behavior of polymers. Depending on the stress history, the polymer can undergo linear viscoelastic, nonlinear viscoelastic, and viscoplastic deformation. The behavior in each regime must be probed using different imposed stress levels and each test is performed over an extended duration. For instance, to calibrate the popular Schapery nonlinear viscoelastic model, a series of creep-recovery tests must be performed at incrementally higher stresses [5,6] beyond the linear limit, each spanning several hours, to adequately represent the nonlinear stress-dependent functions. To measure viscoplastic strains, a long wait time after unloading must be allowed to ensure viscoelastic recovery has ceased and the strain left behind is truly permanent [7–10]. The experimental effort is drastically multiplied when the material in question exhibits anisotropy, and when data need to be obtained as a function of temperature.

The aim of this paper is to establish an experimental method to circumvent the aforementioned obstacle. The proposed method is based on the insight that the number of tests required will be significantly reduced if the strain responses for a range of stress histories can be obtained simultaneously in a single test. This goal can be achieved by using a specimen geometry that creates a known stress gradient, and measuring the corresponding strain distribution over time using a full-field measurement technique, thereby providing a high-throughput test method. While the principle can be applied to any loading modes, we demonstrate it specifically for biaxial tension in polymer membranes in this work.

In the past, commonly used test methods to measure the time-dependent behavior of thin membranes under biaxial stress include the inflated bubble tests (or bulge tests) [9,11] and the inflated cylinder tests [12], where pressurization is employed to stress the membrane in tension. The inflated bubble tests create an equibiaxial state whereas the inflated cylinder tests allow different stress ratios by additionally imposing an axial force along the cylinder. In both methods, the membrane is subjected to a uniform stress field and provides strain information under a single stress only.

We propose the inflated cone method to rapidly accelerate the characterization process. With the cone geometry, varying but known hoop and meridional stress gradients develop along the cone axis under pressurization. The resulting strain fields are measured with three-dimensional digital image correlation (3D-DIC). A rich amount of stress–strain data is collected with respect to time that can be used for constructing viscoelastic and viscoplastic models. The inflated cone method also allows a range of stress ratios to be realized through independently controlling the axial load and hence the meridional stress.

In the following, we first describe the mechanics of the inflated cone and the experimental design. Experiments conducted on low density polyethylene thin film used for superpressure balloon structures are then presented. Finally, the utility of the proposed method is discussed.

2 Inflated Cone Method

A schematic of the inflated cone experiment is shown in Fig. 1. The geometry chosen is a right circular cone where the top and the bottom are clamped onto test fixtures that are connected to a mechanical testing system. A biaxial stress state develops as the cone is pressurized internally and stretched axially.

The stress field of the inflated cone is analyzed using membrane theory. The geometrical parameters and force resultants acting on the membrane are illustrated in Fig. 2. Assuming material isotropy and axisymmetry of the cone is maintained throughout, and the force equilibrium equations are

$$\frac{N_\theta}{r_\theta} + \frac{N_\phi}{r_\phi} = -p \tag{1}$$

$$2\pi R N_\phi \cos\alpha + F = 0 \tag{2}$$

where N_θ and N_ϕ are the force resultants per unit width in the hoop and meridional directions, r_θ and r_ϕ are the principal radii of curvature, p is the internal pressure, α is the cone angle, and F is the external force acting on the cone along the z-axis.

It is possible to separate F into two components: the force due to pressurization and the force applied via mechanical testing machine F_{MTS}. We also assume that the meridional radius of curvature r_ϕ is

[1]Corresponding author.

Contributed by the Applied Mechanics Division of ASME for publication in the Journal of Applied Mechanics. Manuscript received March 4, 2022; final manuscript received May 6, 2022; published online May 17, 2022. Assoc. Editor: Yong Zhu.

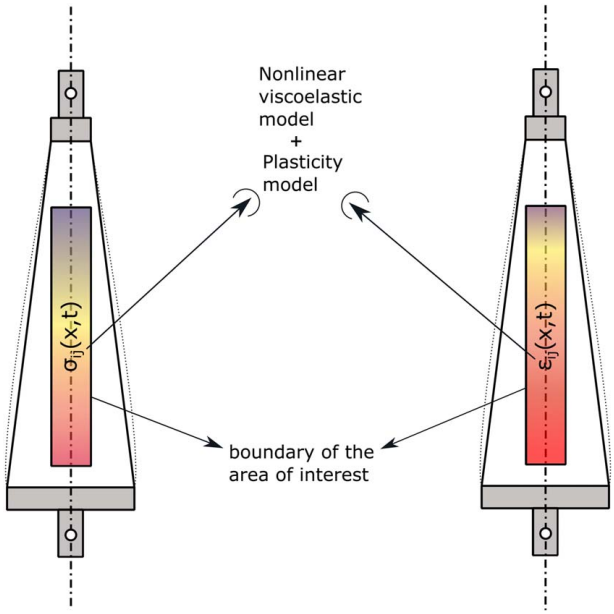

Fig. 1 Schematic of the inflated cone experiment. The strain field, $\varepsilon_{ij}(X, t)$, is obtained by 3D-DIC. Stress and strain fields can be used to construct viscoelastic and viscoplastic models.

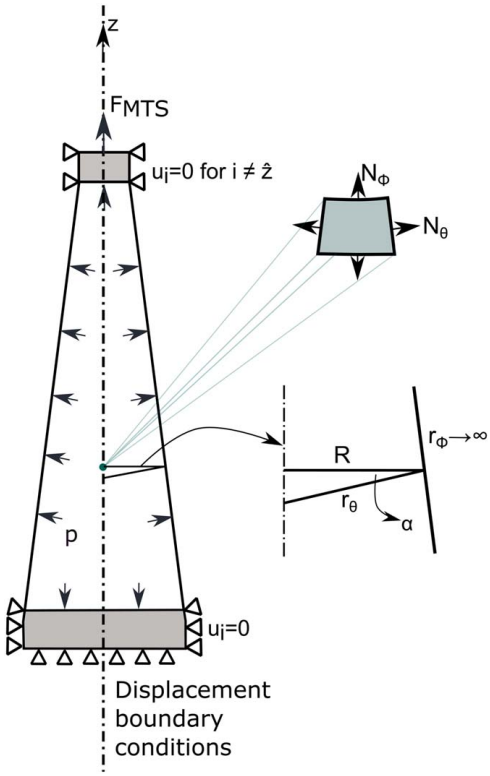

Fig. 2 Boundary conditions of the experimental setup with the notation followed in this study. Lower testing fixture is fixed and upper fixture is free to move in the *z*-direction.

sufficiently large throughout. The hoop stress σ_θ and the meridional stresses σ_ϕ become

$$\sigma_\theta = \frac{pr_\theta}{b} \tag{3}$$

$$\sigma_\phi = \frac{pr_\theta}{2b} + \frac{F_{MTS}}{2\pi r_\theta b \cos^2\alpha} \tag{4}$$

where b is the membrane thickness.

For a given applied pressure p and axial force F_{MTS}, the hoop and meridional stresses vary with the radius of curvature r_θ along any meridian. The stresses are determined from Eqs. (3) and (4) using the measured radii of curvatures from 3D-DIC and the pressure and force sensors. The strains on any points along any meridian on the cone are obtained from 3-D DIC.

The principal stress ratio for nonzero p is given by

$$\frac{\sigma_\phi}{\sigma_\theta}(X, t) = \frac{1}{2} + \frac{1}{2\pi}\left(\frac{F_{MTS}(t)}{p(t)}\right)\left(\frac{1}{r_\theta(X)\cos\alpha}\right)^2 \tag{5}$$

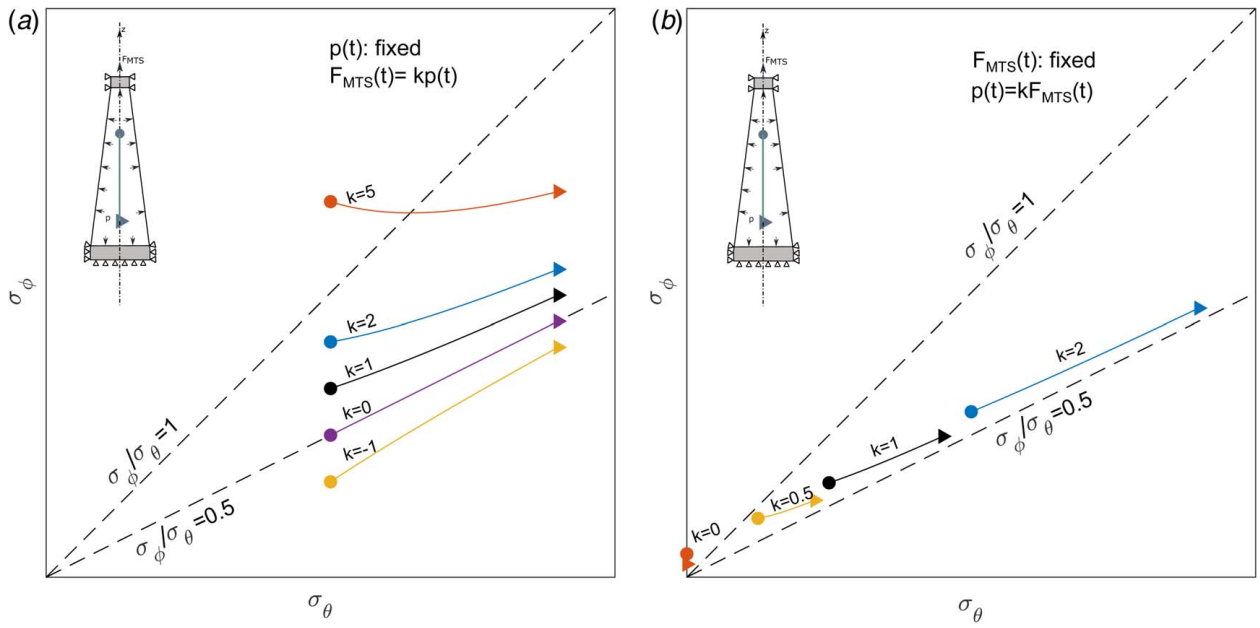

Fig. 3 Effect of experimentally controlled variables, F_{MTS} and p, on the investigated stress states while the geometrical parameters are preserved. Each line represents stress state spectrum obtained by a single inflated cone experiment. The marked points represent the position on the conical specimen. (*a*) Variation of F_{MTS}. (*b*) Variation of p.

Table 1 Cone specimen geometric parameters

Cone height	360 mm
Cone angle, 2α	20°
Base diameter	127 mm
Apex diameter	0 mm

where X denotes the position along any meridian. As seen in Fig. 5, the geometric changes of the cone are small during the experiments. Hence, the temporal dependence of r_θ and α is neglected.

In Eq. (5), the term in the first parenthesis represents experimentally controlled variables whereas the term in the second parenthesis represents geometrical parameters of the specimen. Figure 3 illustrates that the load variables F_{MTS} and p can be varied independently to change the range of stresses (or the principal stress ratio) according to the desired experimental profile. From Eq. (5), it can also be seen that the principal stress ratio reduces to 1/2 for the case of $F_{MTS} = 0$.

3 Experiments

3.1 Cone Specimen Fabrication. StratoFilm 420 (SF420) is used to construct the envelope of the cone. SF420 is a linear low density polyethylene thin film employed in superpressure ballooning applications [11]. It is transparent and has a nominal thickness of 38 μm.

For simplicity, we demonstrate the test method using a full cone rather than a truncated cone. The full cone represents the case of $F_{MTS} = 0$. The conical specimen was manufactured from a flat SF420 sheet as follows. A mask with the shape of a developed half-cone was first prepared and placed onto the SF420 to provide the cutting pattern. Two halves (front and back) of the cone envelope were then cut from the SF420 sheet using a precision cutter and sealed with an impulse heater for 3 s along two seam lines. The width of the seams was 2 mm. The front face of the cone was lightly sprayed with black paint to achieve desirable contrast for 3D-DIC. To minimize the influence of the seams, the region for strain inspection was chosen to be away from the seams. In addition, the seam width was kept as low as possible compared to the cone base diameter.

The dimensions of the conical specimen used in this study are summarized in Table 1. The selection of the geometric parameters can be varied according to the available size of the experimental setup. One thing to note is that the stress gradient can be varied along any meridian by changing the cone angle α.

3.2 Experimental Setup and Procedure. The experimental configuration is illustrated in Fig. 4. A BMP280 absolute barometric pressure sensor was placed inside the cone. To inflate the specimen, we used the laboratory air supply and reduced the output pressure to an experimentally desirable level via a pressure regulator. A microcontroller was used for controlling the solenoid valve and logging the pressure sensor data. The solenoid valve used on–off control for modulating the pressure inside the cone. The random black pattern on the front face of the conical specimen was illuminated by diffused white light panel located behind the specimen to obtain optical contrast in images. Data acquisition rate was set to 1 Hz for the pressure sensor and images were taken at every 15 s using a Correlated Solutions 3D-DIC system. A small subset size of 35 pixels, which corresponds to approximately 2.5 mm, was used in the DIC analysis.

The loading profile consisted of four distinct stages: inflation, constant pressure, deflation, and zero-pressure recovery. The first two stages of the experiment were 60 min each and the recovery period after quick deflation was 280 min. Before the experiment, the reference image was captured after applying a small differential pressure to give the specimen its initial form. During inflation, we applied stepwise pressure increments of 100 Pa for every 60 s until the desired hold pressure of 5.3 kPa was reached.

Fig. 4 Experimental setup for the inflated full cone ($F_{MTS} = 0$) used in this study. The bottom of the cone was secured to the testing fixture with closed cell foam tape and hose clamps.

4 Results and Discussion

4.1 Stress and Strain Histories. The curvatures measured at ten inspection points along the selected meridian are shown in Fig. 5. The maximum principal curvature, $\kappa_\phi = 1/r_\phi$, of these points is close to zero as expected. The minimum principal curvature, $\kappa_\theta = 1/r_\theta$, changes continuously along the meridian. The hoop and meridional stress histories calculated using Eqs. (3)

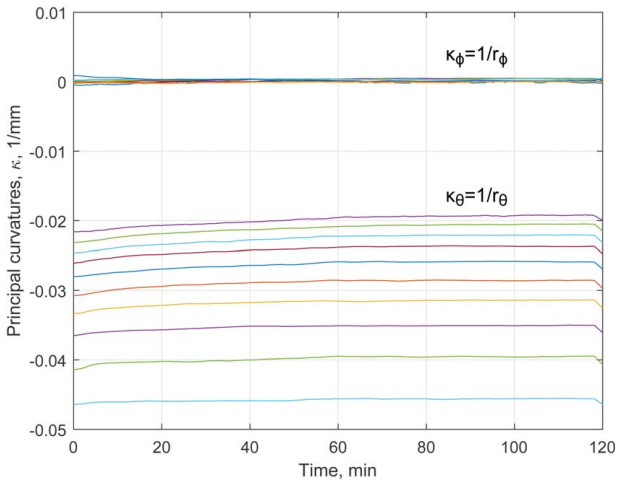

Fig. 5 The principal curvatures obtained from DIC. The first principal curvature, κ_ϕ, values at the inspection points are minimal and accepted as zero in subsequent analyses.

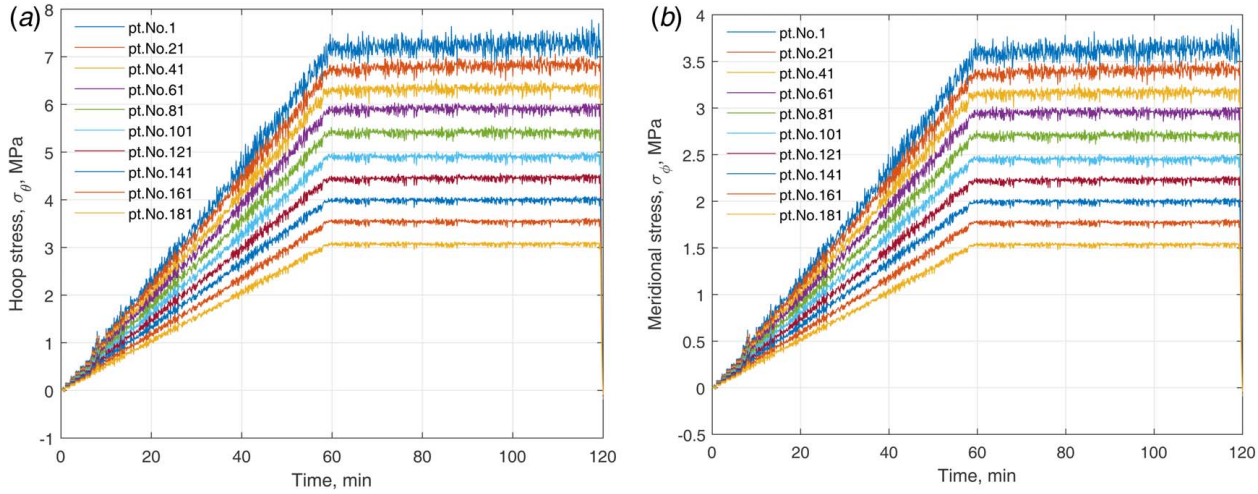

Fig. 6 The calculated stress field from the pressure and curvature values for ten selected inspection points: (*a*) hoop stress history and (*b*) meridional stress history

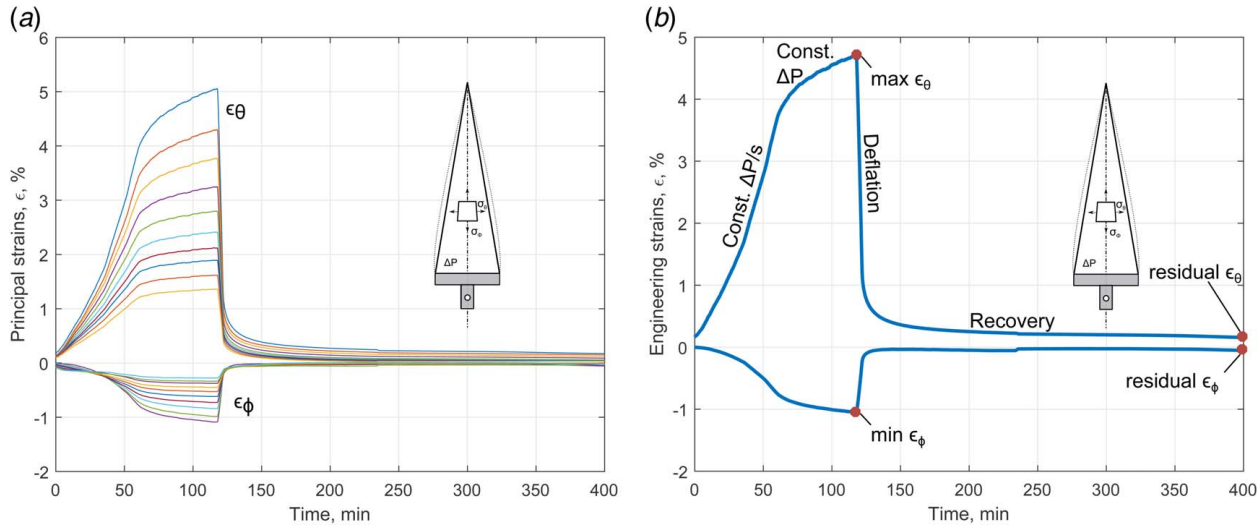

Fig. 7 (*a*) Strain history of the ten inspection points in Fig. 6, including the recovery period of 280 min. (*b*) Strain history of an isolated point displaying the loading and recovery profile with marked points of interest.

and (4) are shown in Fig. 6. Since the applied axial load is zero, the principal stress ratio is 1/2 for all sampling points.

The measured principal strain histories for the same inspection points are shown in Fig. 7. The principal strain fields, similar to stress field, vary continuously in two principal directions. It can be observed that SF420 displays considerable strain increase over time during constant stress and strain recovery after unloading. Figure 8 shows the corresponding creep compliances for the selected inspection points during the experimental duration. The proposed inflated cone method has the obvious advantage of generating a continuous range of compliances with a single experiment.

4.2 Residual Strains. In determining the yielding onset and permanent strain of polymers, the residual strain method [8] is commonly employed by researchers. The residual strain method requires stressing (straining) the material up to various stresses (strains) and recording the residual strains. If sufficient time is allowed during free recovery, the residual strains can be accepted as irrecoverable plastic strains [7].

Figure 9 displays the inspection line (front meridian) containing 200 inspection points together with minimum and maximum

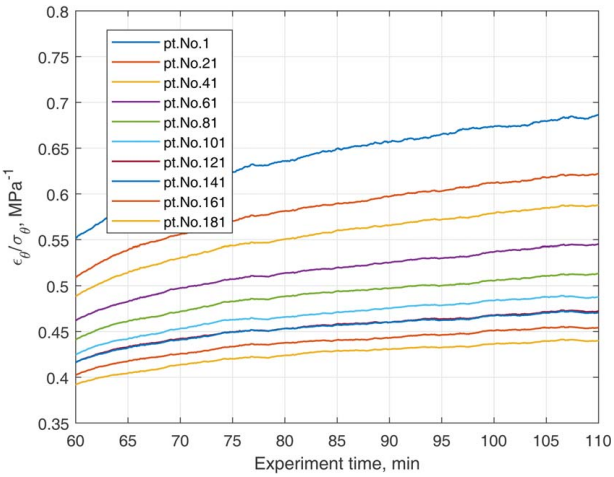

Fig. 8 Creep compliances, $\varepsilon_\theta/\sigma_\theta$, shown for different inspection points (corresponding to different stresses) during the creep period

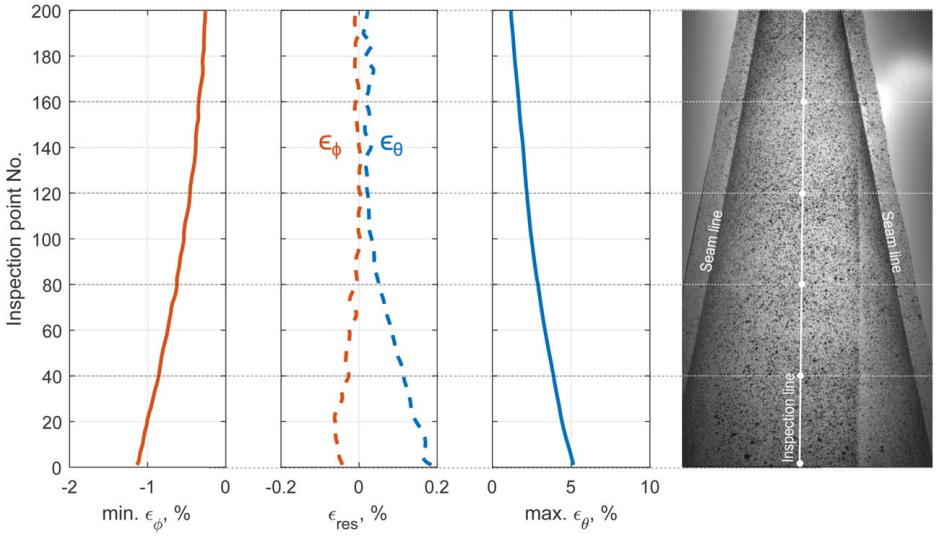

Fig. 9 Minimum meridional and maximum hoop strains and their corresponding residual strains for 200 inspection points are shown with the inspection line containing the inspection points

principal strains of these points during the experiment and their corresponding residual strains. As it can be seen, larger experimental strains (i.e., points located lower on the meridian) correspond to larger residual strain readings. In a single experiment, a spectrum of residual strains and trends can be obtained.

5 Concluding Remarks

Characterization of long-term time-dependent mechanical behavior of polymers in the nonlinear regime is time-consuming due to the need of repeated testing at different stress levels. We have presented an experimental method capable of generating strain responses over time under a range of stress in a single experiment. The underlying principle is to apply a nonuniform but known stress field via a varying specimen geometry and to measure the resulting nonuniform strain distribution by a full-field measurement technique.

We have demonstrated the principle on polymer membranes under biaxial stress using an inflated cone and utilized three-dimensional digital image correlation for full-field strain measurement. The inflated cone test is significantly more efficient than the commonly used inflated bubble or inflated cylinder tests. Instead of obtaining discrete data points, each inflated cone experiment provides a spectrum of data points. The stress ratio and range can be flexibly modified by changing the cone geometry and applied loads.

The inflated cone method is a powerful technique that accelerates time-dependent characterization for polymer membranes and is especially valuable for gathering data for nonlinear viscoelastic modeling, yielding onset determination, and viscoplastic modeling.

The method can be readily extended to anisotropic membranes where the material directions coincide with the meridional and hoop directions of the cone. If this condition is not satisfied, the deformation ceases to be axisymmetric under inflation. The procedure to determine the hoop and meridional stresses need to be modified. In particular, the hoop curvature variation along the hoop direction needs to be measured and taken into account to calculate the correct stresses.

Acknowledgment

We are grateful for the financial support from the NASA Goddard Space Flight Center (Grant No. 80NSSC21K0913). We thank the NASA Balloon Program Office and Tensys Dynamics Limited for helpful comments and discussion.

Conflict of Interest

There are no conflicts of interest.

Data Availability Statement

The datasets generated and supporting the findings of this article are obtainable from the corresponding author upon reasonable request.

References

[1] Cathey, H., 2009, "The NASA Super Pressure Balloon – A Path to Flight," Adv. Space Res., **44**(1), pp. 23–38.
[2] Schenk, M., Viquerat, A. D., Seffen, K. A., and Guest, S. D., 2014, "Review of Inflatable Booms for Deployable Space Structures: Packing and Rigidization," J. Spacecr. Rockets, **51**(3), pp. 762–778.
[3] Johnson, L., Whorton, M., Heaton, A., Pinson, R., Laue, G., and Adams, C., 2011, "NanoSail-D: A Solar Sail Demonstration Mission," Acta Astronaut., **68**(5–6), pp. 571–575.
[4] Datashvili, L., 2010, "Multifunctional and Dimensionally Stable Flexible Fibre Composites for Space Applications," Acta Astronaut., **66**(7–8), pp. 1081–1086.
[5] Schapery, R. A., 1969, "On the Characterization of Nonlinear Viscoelastic Materials," Polym. Eng. Sci., **9**(4), pp. 295–310.
[6] Zhang, L., Klimm, W. J., Kwok, K., and Yu, W., 2022, "A Nonlinear Viscoelastic–Viscoplastic Constitutive Model for Epoxy Polymers," AIAA SCITECH 2022 Forum, San Diego, CA, Jan. 3–7, American Institute of Aeronautics and Astronautics.
[7] Quinson, R., Perez, J., Rink, M., and Pavan, A., 1996, "Components of Non-Elastic Deformation in Amorphous Glassy Polymers," J. Mater. Sci., **31**(16), pp. 4387–4394.
[8] Quinson, R., Perez, J., Rink, M., and Pavan, A., 1997, "Yield Criteria for Amorphous Glassy Polymers," J. Mater. Sci., **32**(5), pp. 1371–1379.
[9] Bosi, F., and Pellegrino, S., 2017, "Molecular Based Temperature and Strain Rate Dependent Yield Criterion for Anisotropic Elastomeric Thin Films," Polymer, **125**, pp. 144–153.
[10] Ozdemir, V. B., and Kwok, K., 2021, "Time-Dependent Yielding of Polymer Thin Films Under Creep," Conference Proceedings of the Society for Experimental Mechanics Series, Vol. 2, pp. 5–16.
[11] Li, J., Kwok, K., and Pellegrino, S., 2016, "Thermoviscoelastic Models for Polyethylene Thin Films," Mech. Time-Dependent Mater., **20**(1), pp. 13–43.
[12] Kwok, K., and Pellegrino, S., 2011, "Large Strain Viscoelastic Model for Balloon Film," 11th AIAA Aviation Technology, Integration, and Operations (ATIO) Conference, Virginia Beach, VA, Sept. 20–22, American Institute of Aeronautics and Astronautics.